Neurocrit Care (2022) 37:S206–S219
https://doi.org/10.1007/s12028-022-01491-6

NEUROCRITICAL CARE SOCIETY

BIG DATA IN NEUROCRITICAL CARE

Leveraging Continuous Vital Sign Measurements for Real-Time Assessment of Autonomic Nervous System Dysfunction After Brain Injury: A Narrative Review of Current and Future Applications

Jamie Podell[1,2], Melissa Pergakis[1,2], Shiming Yang[3], Ryan Felix[1], Gunjan Parikh[1,2], Hegang Chen[4], Lujie Chen[5], Catriona Miller[6], Peter Hu[1,3] and Neeraj Badjatia[1,2,7*]

Abstract

Subtle and profound changes in autonomic nervous system (ANS) function affecting sympathetic and parasympathetic homeostasis occur as a result of critical illness. Changes in ANS function are particularly salient in neurocritical illness, when direct structural and functional perturbations to autonomic network pathways occur and may herald impending clinical deterioration or intervenable evolving mechanisms of secondary injury. Sympathetic and parasympathetic balance can be measured quantitatively at the bedside using multiple methods, most readily by extracting data from electrocardiographic or photoplethysmography waveforms. Work from our group and others has demonstrated that data-analytic techniques can identify quantitative physiologic changes that precede clinical detection of meaningful events, and therefore may provide an important window for time-sensitive therapies. Here, we review data-analytic approaches to measuring ANS dysfunction from routine bedside physiologic data streams and integrating this data into multimodal machine learning–based model development to better understand phenotypical expression of pathophysiologic mechanisms and perhaps even serve as early detection signals. Attention will be given to examples from our work in acute traumatic brain injury on detection and monitoring of paroxysmal sympathetic hyperactivity and prediction of neurologic deterioration, and in large hemispheric infarction on prediction of malignant cerebral edema. We also discuss future clinical applications and data-analytic challenges and future directions.

Keywords: Autonomic nervous system, Machine learning, Traumatic brain injury, Ischemic stroke, Neurological decline

Introduction

The autonomic nervous system (ANS) regulates involuntary physiologic processes of cardiovascular function, respiration, and digestion via a widespread neural network. The ANS is divided into the parasympathetic, sympathetic, and enteric divisions differentiated by their conservation or expenditure of energy. Sympathetic and parasympathetic divisions have afferent and efferent

*Correspondence: NBadjatia@som.umaryland.edu
[7] Shock Trauma Neurocritical Care, University of Maryland Medical Center, 22 S. Greene Street, G7k19, Baltimore, MD 21218, USA
Full list of author information is available at the end of the article

Springer

fibers to the central nervous system ensuring the careful modulation of target organs for physiologic homeostasis. Supraspinal control of autonomic function is modulated by the brainstem, hypothalamus, and cortical centers forming a carefully regulated neural network controlling vital functions [1].

Autonomic control of the cardiovascular system requires precise neural regulation. Sensory information relating to cardiovascular function is conveyed by changes in baroreceptors and chemoreceptors. Baroreceptors, which sense a change in pressure in vessel walls, are found in the carotid sinus and aortic arch. Chemoreceptors, which are affected by changes in the partial pressure of oxygen and carbon dioxide, are found in the carotid bodies and the aorta. Both relay information to the hypothalamus via the vagus nerve and solitary tract nucleus in the medulla. Based on the afferent input, smooth and cardiac muscles are activated via the visceral motor pathway to respond accordingly, balancing sympathetic and parasympathetic drive and maintaining homeostatic function of cardiac output and vascular tone. The nucleus ambiguous and dorsal vagal nucleus provide parasympathetic input to the heart via the vagus nerve, whereas sympathetic input travels via neurons in the intermediolateral column at T1 to T5 of the spinal cord and is modulated by the ventrolateral medulla and paraventricular nucleus of the hypothalamus [2].

Higher cortical input from the insula and other forebrain regions also play vital, yet complex, roles in the modulation of sympathetic and parasympathetic output; meta analyses of lesion studies and neural network mapping have identified a central autonomic network connecting insular, prefrontal, and cingulate cortices, amygdala, hippocampus, hypothalamus, and thalamus with projections to medullary and spinal nuclei controlling cardiac function [3–6]. Cardiovascular autonomic control is derived from reciprocal connections to target organs through the peripheral nerves, spinal cord, brainstem, and cortical and subcortical brain areas. Disruption anywhere along these pathways, as occurs in neurocritical illness, can alter autonomic homeostasis resulting in measurable cardiovascular physiologic changes [7–9].

Autonomic dysfunction has been described in a across many nonneurologic disease states such as sepsis [10], acute myocardial infarction [11], and traumatic shock [12]. It has been shown to be a predictor of mortality in patients with myocardial infarction [13] and chronic heart failure [14]. Critically ill pediatric and adult patients with sepsis have separately been shown to have autonomic dysfunction that is inversely related to disease severity and subsequently improves in the recovery state [15–17]. Autonomic dysfunction in critical illness, as exemplified in sepsis, is likely due to the maladaptive response of the body to physiologic distress leading to prolonged sympathetic activation and an imbalance between sympathetic and parasympathetic output [18]. Studies of patients with brain injury have shown similar findings of autonomic dysfunction [19–24]. Given the various neuroanatomic regions of autonomic control susceptible to injury due to trauma, stroke, hemorrhage, and inflammatory processes, autonomic dysfunction phenotypes are of particular interest in neurocritical care as potential markers of disease severity or predictors for neurological deterioration. To this end, quantitative physiologic modeling of ANS function may represent a promising and underused tool in neurocritical care.

Modeling ANS with Continuous Vital Signs

Signal Processing

Real-time assessment of the ANS signal can be performed by leveraging continuous data streams of vital signs from bedside monitors. At our institution, each patient monitor collects real-time 240-Hz waveforms and 0.5-Hz data trends, which are transferred via secure intranet to a dedicated server and archived [25]. Physiological data collected through this system include electrocardiographic (ECG), photoplethysmography (PPG), carbon dioxide, arterial blood pressure, and intracranial pressure (ICP) waveforms. Data trends include heart rate (HR), respiratory rate (RR), temperature, oxygen saturation, end-tidal carbon dioxide, ICP, as well as any other continuous monitoring device that can interface with our bedside monitoring system (GE Marquette-Solar-7000/8000; General Electric, Fairfiled, CT).

In addition to continuous physiologic data, information with different formats and temporal resolutions can be collected and used for analysis. These include ordinal or categorical data (e.g., Glasgow Coma Scale [GCS], age, sex), radiological images, text (medical records, clinical notes), and other relevant data (adverse events, treatments, laboratory tests, etc.).

Validated and automated medical data processing techniques may distill useful information from the above-generated massive amounts of data. Such processed data can be used either directly by clinicians to recognize physiological changes or pipelined to predictive models for algorithmic-assisted decision making. Automated decision support tools may enhance clinicians' capacity to interpret complex, multimodal patient data. Although continuous ICP and electroencephalogram (EEG) monitors are often used in neuroscience intensive care units (ICUs), they may not be clinically indicated in all patients. Similarly, continuous blood pressure monitoring via invasive arterial lines can be used for assessment of blood pressure variability in select populations.

However, noninvasive ECG and PPG sensors are applied to all critical care patients and thus are crucial for generalizable physiologic models.

HR variability (HRV), derived from the ECG waveform, refers to several features calculated from a set of methods evaluating beat-to-beat changes in the heart rhythm, and has long been used to evaluate cardiac autonomic function associated with neurological disorders [26–28]. As described, autonomic dysfunction is a potential complication following acute brain injury such as severe traumatic brain injury (TBI) [29], where quantitative changes in HRV can occur. For example, in the work by Baguley et al. [30], patients with and without dysautonomia showed different HRV responses to afferent stimuli following TBI. Further, HRV is often used as the preferred method to assess autonomic dysfunction in general critical illness including sepsis [15–17].

In calculating HRV features from bedside ECG monitoring systems, data preprocessing, including detection and removal of artifacts, must first occur. To this end, we initially filter out extreme values that are outside of the sensor's measurement range. Next, we apply robust smoothing algorithms to reduce noise [31, 32]. Finally, we identify QRS peaks from the ECG. Figure 1 shows a typical PQRST segment, which identified a pair of consecutively identified R peaks. Automated identification of these peaks occurs by searching all local maxima and setting physiologically reasonable parameters to detect R peaks by following a few simple rules [33]. For example, the minimal distance between adjacent R peaks can be restricted by the maximum possible HR (e.g., 200 bpm), and a point may qualify as an R peak if its prominence is higher than a threshold (empirically determined as half of typical peak-valley distance), so that flat signals with small fluctuations will not be included. Standard Python library was used for peak detection (Scipy v.1.5.2). Z-scores are calculated for detected normal-to-normal (NN) intervals and intervals with a z-score larger than 3 are removed. Additionally, sophisticated algorithms such as the Pan Tompkins method may be used [34]. This automatically preprocessed data generates NN intervals.

From the above derived NN intervals, HRV features in time domain, frequency domain, and nonlinear dynamics can be calculated based on the Task Force of the European Society of Cardiology and the North American Society of Pacing and Electrophysiology [13]. Table 1 lists common HRV features and their definitions. Time domain features are the simplest features, representing statistical summaries of the RR interval length (Fig. 1a), and they can be calculated over short (e.g., 5 min) or long (e.g., 24 h) time periods. Applied clinically, reduced time domain HRV has been observed in several neurological and nonneurological diseases [13].

Frequency domain features are derived from the HRV power spectrum analysis and focus on the differential contributions of sympathetic and parasympathetic divisions of the ANS on heart rate. There are four components used in calculating frequency domain HRV, including ultra very low frequency (LF) (0–0.003 Hz), very LF (0.003–0.04 Hz), LF (0.04–0.15 Hz), and high frequency (HF) (0.15–0.4 Hz) power. Figure 1c and d show the power spectrum density calculated by the Welch and Lomb methods, respectively. The HF component is related to the parasympathetic system [13], and the LF/

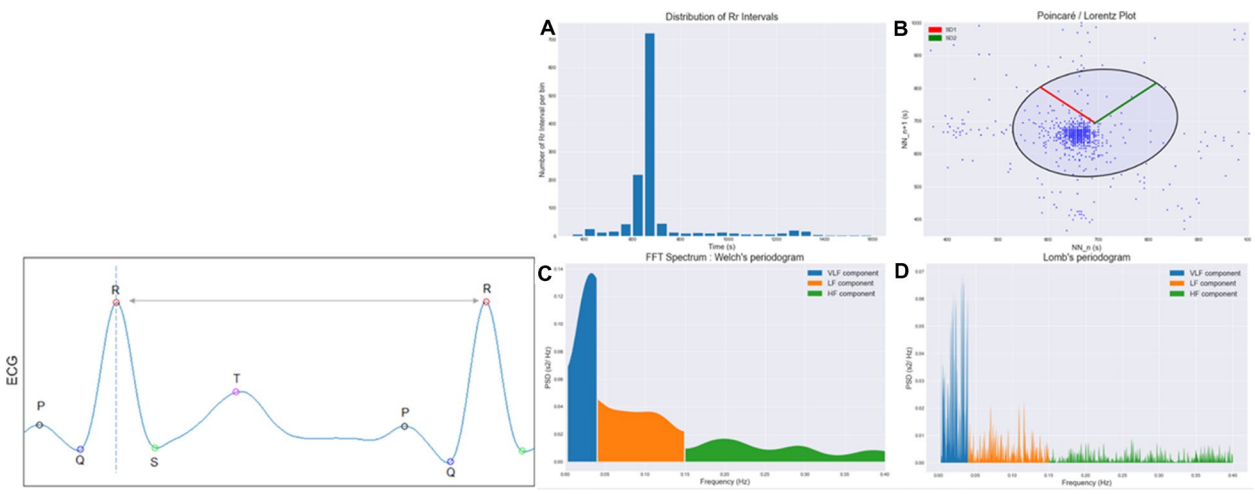

Fig. 1 Illustration of ECG segment with detected P, Q, R, S, T, and R-R interval. Plots of HRV features. **a** Distribution of R–R intervals. **b** Poincare plot for nonlinear domain features. **c** The power spectrum density plot for frequency domain features using Welch's method. **d** The power spectrum density plot for frequency domain features using Lomb's method. ECG, electrocardiography, HRV, heart rate variability (color figure online)

Table 1 Common HRV variables and their definitions

HRV vVariable	Definition	Unit
Time domain		
Mean NN	Mean NN intervals	ms
SDNN	Standard deviation of NN intervals	ms
RMSSD	Root mean square of the sum of the squares of differences between adjacent NN intervals	ms
SDNN index	Mean of the SDNN values of each 5-min segment	ms
pNN50	Percentage of NN intervals that differences between adjacent NN intervals > 50 ms	%
pNN20	Percentage of NN intervals that differences between adjacent NN intervals > 20 ms	%
Frequency domain		
Total power	Spectral power of NN intervals 0 to — 0.4 Hz	ms^2
UVLF	Spectral power of NN intervals 0–0.003 Hz	ms^2
VLF	Spectral power of NN intervals 0.003 to — 0.04 Hz	ms^2
LF	Spectral power of NN intervals 0.04 to — 0.15 Hz	ms^2
HF	Spectral power of NN intervals 0.15 to — 0.4 Hz	ms^2
LF/HF	Ratio of LF to HF power	–
Nonlinear dynamics		
SD1	Standard deviation of the Poincare plot (PP) perpendicular to the line of identity	ms
SD2	SD of the PP along the line of identity	ms
SD2/SD1	Ratio of SD2 to SD1	–
Alpha1	Short term fluctuation slope in detrended fluctuation analysis	–
Alpha2	Long term fluctuation slope in detrended fluctuation analysis	–
Ellipse area	Area of the ellipse fit of PP	–

HF high frequency, *HRV* heart rate variability, *LF* low frequency, *NN* normal-to-normal, *PP* Poincare plot, *SD1* standard deviation of the Poincare plot perpendicular to the line of identity, *SD2* standard deviation of the Poincare plot long the line of identity, *SDNN* standard deviation of normal-to-normal intervals, *UVLF* ultra very low frequency, *VLF* very low frequency

HF ratio has been used to quantify the changing relationship between sympathetic and parasympathetic activities [35], with controversy as to whether it is an accurate measure of cardiac sympatho-vagal balance [32]. Additional methods for assessing the ANS measure nonlinear dynamic features of HRV. Nonlinear dynamic methods were designed to capture the complex, dynamic interactions between heart rhythm, respiration, and hemodynamic states. They include measures of signal entropy, fractal correlation properties, and mathematical descriptors of the Poincare plot (PP) [36–38]. The PP describes the dependence between successive NN intervals and is graphically displayed in Fig. 1b. An ellipse is fitted to the plot which generates two parameters: standard deviation of the PP perpendicular to the line of identity and standard deviation of the PP long the line of identity. Nonlinear dynamics features have been used in predicting vascular events for hypertensive patients [39], need for blood transfusions in patients with trauma [40], and secondary neurological deterioration after TBI [41].

Data Visualization

Significant amounts of unprocessed data may lead to cognitive overload for ICU clinicians responsible for patients with multiple complex acute and nonacute medical problems. An automated physiological data-organizing and information-summary system can present aggregated information from multiple data sources, provide at-a-glance summaries of clinical data, and assist with prioritizing care for multiple patients. A longitudinal display of vital sign patterns may improve patient assessment and clinical decision making. Figure 2 demonstrates a patient's 12-hour vital sign (VS) trajectories using a data visualization tool or "viewer" aimed to achieve this goal. VS in normal ranges is displayed in green. Yellow and red colors are used to highlight VS segments in abnormal ranges. Those ranges are predefined based on clinical consensus. In the right panel, two two-dimensional plots show the longitudinal changes of systolic blood pressure versus HR, and cerebral perfusion pressure versus ICP (blue, 12 h ago, red, recent). If the points in the two-dimensional diagrams move toward the bottom right (or top left) corner, it may suggest the patient has deteriorated (or ameliorated) bleeding issue or neurologic issue.

In addition to visualizing real-time vital sign trends, our viewer can serve as a platform to display relevant data transformations and decision support tools. For example, we can display real-time cerebrovascular pressure-reactivity index (PRx) alongside other VS, showing instant relationships between hemodynamic changes and

Fig. 2 ICU vital sign viewer. Real-time display of 12 hour of continuous vital sign data with color coded values based on predefined thresholds. This display includes calculated values such as the shock index (SI) and cerebrovascular autoregulation (PRx). In the far right panel, cross relationship between systolic blood pressure and heart rate as well as CPP and ICP are displayed with color-coding indicating the time data were acquired (blue, 12 h ago, red, current). *CPP* cerebral perfusion pressure, *ICP* intracranial pressure, *ICU* intensive care unit (color figure online)

cerebrovascular autoregulation. PRx has been proposed as an indicator of loss of autoregulatory reserve [42] and is calculated as a moving correlation coefficient between the mean arterial pressure (MAP) and ICP. Given a short time window, about 40 consecutive averaged MAP and ICP in 4–5 min are used for calculation [43]. When cerebral autoregulation is intact, CBF does not change significantly with mean blood pressure. In this situation, calculated PRx should be close to zero showing weak correlation between MAP and ICP. When cerebral autoregulation is impaired after severe head injury, CBF increases or decreases with blood pressure, and the absolute value of PRx moves away from zero indicating a strong linear correlation between MAP and ICP.

Clinical Examples

The real-time physiologic data viewer may also be programed to demonstrate clinically relevant risk scores derived from validated data-derived mathematical models. Such model outputs may represent specific dysautonomia phenotypes associated with risk for neurologic deterioration in different clinical scenarios such as TBI or large hemispheric infarct (LHI), or they may alert clinicians to physiologic syndromes such as paroxysmal sympathetic hyperactivity (PSH) after TBI or evolving neurogenic shock after spinal cord injury (SCI). Details regarding such clinical applications are provided below.

Paroxysmal Sympathetic Hyperactivity (PSH)

Paroxysmal sympathetic hyperactivity is a prototypical example of clinically relevant dysautonomia in neurocritical illness, fundamentally characterized by an imbalance between the sympathetic and parasympathetic nervous systems resulting in recurrent episodes of hypertension, tachycardia, hyperthermia, diaphoresis, and motor rigidity, with numerous deleterious downstream effects [44, 45]. Although it can occur in a variety of clinical scenarios, it is most often reported following moderate to severe acute TBI, in upwards of one third of critically ill patients beginning around the second week of hospitalization [44–50]. TBI-related PSH appears to be both a marker of injury severity and an independent risk factor for poor outcome [47, 51]. As such, it may represent a promising treatment target to mitigate secondary morbidity in

at-risk patients. However, its potential in this regard has been limited by prevailing diagnostic uncertainty, under-recognition, and a lack of reliable quantitative detection and monitoring tools. Treatments are often reactive to the most extreme physiologic derangements and therefore delayed past a critical window for mitigating secondary injury. In 2014, an expert consensus-based PSH assessment measure (PSH-AM) standardized terminology, clinically defined PSH, and proposed a quantitative metric for PSH diagnostic likelihood and symptom severity (Table 2) [44]. Several subsequent studies have validated the PSH-AM as a sensitive but not specific tool for PSH diagnosis [49, 50], but a number of limitations have impeded its widespread adoption and utility as a quantitative detection and monitoring tool. For example, tabulation of the PSH-AM requires manual information gathering often limited by incomplete documentation, continued reliance on subjective clinical inference and the exclusion of other causes, and a one-size-fits-all approach to VS derangements. High-resolution physiologic data streams capable of probing the integrity of the autonomic nervous syndrome remain underused.

At present, no studies have attempted to mathematically model the physiologic derangements characteristic of PSH. However, hypothesis-generating studies investigating objective physiologic features associated with clinically defined PSH are emerging. For example, a study by Baguley and colleagues [52] predating the PSH-AM compared patients with TBI without transient sympathetic arousals versus with transient sympathetic arousals and persistent dysautonomia, finding that at seven days post injury there were no differences in standard physiologic measurements at rest, but physiologic responses to nociceptive stimulation diverged between groups. Specifically, they observed a decrease in HRV features including HF power and LF/HF ratio and greater increases in HR compared with baseline in patients with TBI with sympathetic arousals, especially in those who went on to show persistent evidence of dysautonomia at 2 weeks post injury. Other studies have identified early physiologic predictors of clinically defined PSH including fever

Table 2 Paroxysmal sympathetic hyperactivity-assessment measure (PSH-AM)

Clinical feature scale (CFS)	0	1	2	3	Score
Clinical feature scale (CFS)					
Heart rate	< 100	100 to — 119	120 to — 139	≥ 140	
Respiratory rate	< 18	18 to — 23	24 to — 29	≥ 30	
Systolic blood pressure	< 140	140 to 159	160 to — 179	≥ 180	
Temperature	< 37	37 to — 37.9	38 to — 38.9	≥ 39	
Sweating	Nil	Mild	Moderate	Severe	
Posturing during episodes	Nil	Mild	Moderate	Severe	
CFS subtotal					
Diagnosis likelihood tool (DLT); score 1 point for each feature present					
Clinical features occur simultaneously					
Episodes are paroxysmal in nature					
Sympathetic over-reactivity to normally non-painful stimuli					
Features persist ≥ 3 consecutive days					
Features persist ≥ 2 weeks					
Features persist despite treatment of alternative differential diagnoses					
Medication administered to decrease sympathetic features					
≥ 2 episodes daily					
Absence of parasympathetic features during episodes					
Absence of other presumed cause of features					
Antecedent acquired brain injury					
DLT subtotal					
Combined total (CFS + DLT)					
PSH diagnostic likelihood			Unlikely		< 8
			Possible		8 to — 16
			Probable		> 17

PSH paroxysmal sympathetic hyperactivity

[53] and higher systolic blood pressure [47]. In combination with rules derived from clinical PSH criteria, these findings may aid in the development of machine learning models for automatic PSH detection and quantification.

A major challenge in building such machine learning models is that labels of positive and negative PSH (i.e., episodes with or without PSH) instances are not present naturally in the dataset, and diagnostic uncertainty makes expert rules and ground truths difficult to obtain. This is in contrast to well-defined clinical end points used for the development of early warning scores [54] and for prediction of discrete outcomes. In addition to population-based studies, exploratory visualization of high resolution multimodal physiologic data from prototypical patients also may be used to generate hypotheses for building machine learning models and pathophysiologic theories. For example, Fig. 3 shows exploratory power spectral densities over time in a prototypical patient with TBI with PSH (top panel) versus without (bottom panel), demonstrating higher power very LF (> 8-h period) variation in HR and systolic blood pressure over time in the patient with PSH. Machine learning for PSH detection can incorporate such hypothesis using weak supervision [55, 56] and active learning [57, 58] approaches that leverage data visualization tools, expert review, and PSH-AM scores as noisy approximations to ground truths. Weakly supervised machine learning allows for initial imprecise labeling of training data (which can account for PSH diagnostic uncertainty), and active learning involves an iterative process of machine-generated label refinement by an expert. These approaches necessitate collaboration between clinician "experts" and data scientists. In an example data-analytic pipeline, we are exploring an event mining framework [59] to identify defining features of PSH from each data stream, including paroxysmal (sudden onset) and transient (short duration) characteristics, using unsupervised anomaly detection methods [60–63]. Anomaly detection first estimates a stable personalized baseline for each data stream followed by identifying a list of deviating events, which may be fused to check for simultaneity across multiple parameters (another component of PSH diagnostic criteria). Interpretable machine learning methods such as temporal rule learning [64] may also be used to derive an initial

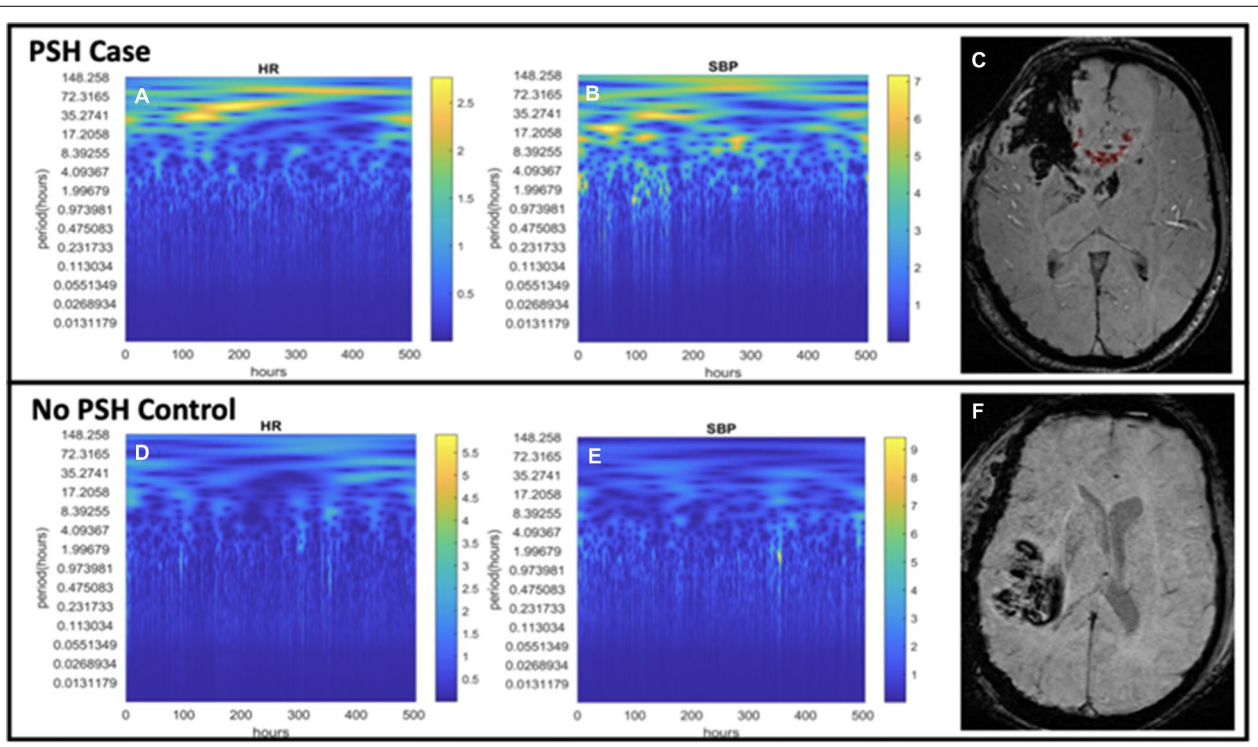

Fig. 3 Physiologic and anatomic correlates of PSH. Continuous vital sign wavelet transformation modeling and representative susceptibility-weighted magnetic resonance imaging axial slices from patients with traumatic brain injury (TBI) with (upper panel) and without (lower panel) paroxysmal sympathetic hyperactivity (PSH). **a**, **b** Represent power spectral analyses of heart rate (HR) and systolic blood pressure (SBP) fluctuations, respectively, over different periods across time, demonstrating high power in very low frequency (long period) bands in a patient with PSH, whereas **d** and **e** demonstrate the absence of high power low frequency fluctuations in a patient with TBI without PSH. **c** Demonstrates frontal hemorrhagic contusions and traced lesions within the corpus callosum region of interest in a patient with PSH. **f** Demonstrates similar hemorrhagic contusion pathology without lesions in the corpus callosum in a patient with TBI without PSH (color figure online)

set of rules. Models of higher complexity such as random forests and deep learning architectures such as ResNets [65] may further refine these rules, which will ultimately generate annotations for expert visualization and validation (Fig. 4). Validated rules may be used to automatically produce labels to be used to build supervised machine learning models to generate output in the form of a continuous PSH index score, which can be further refined to describe multidimensional features of PSH, such as frequency, duration, and magnitude.

Once a quantitative PSH index has been derived, analyses of its clinical validity, use, and pathophysiologic associations can proceed in a relatively straight-forward manner. In addition to providing an intermediate endpoint important for future clinical trials, the PSH index may better clarify neuroanatomic and neurophysiologic correlates of PSH, which in turn may lead to the development of alternative mechanistically grounded therapies. Initially conceptualized as "diencephalic autonomic epilepsy" [66] theories regarding the pathophysiology of PSH have evolved over time, with the most accepted contemporary theories proposing that structural and functional damage to the central autonomic network lead to a final common pathway explained by the excitatory-inhibitory ratio model [45]. This theory posits that sympathetic paroxysms are driven by disconnection of inhibitory pathways to the brainstem and spinal cord, where maladaptive dendritic arborization leads to overexcitable sympathetic circuits with diminished capacity for higher control of inappropriate physiologic responses to stimuli [45]. Radiographically, diffuse axonal injury is most commonly reported [19, 50, 53, 67], in concordance with such disconnection models. In an age-matched and GCS-matched PSH case–control study, our group found that initial computed tomography (CT) imaging findings of diffuse axonal injury, complete cisternal effacement, SAH/IVH, and absence of focal contusions were associated with higher risk for inpatient development of PSH [47]. Additionally, a magnetic resonance imaging diffusion tensor imaging(DTI) study found that decreased fractional anisotropy (FA) in the posterior limb of the internal capsule and the splenium of the corpus callosum could distinguish PSH from non-PSH cases [53]. Our preliminary work investigating clinical magnetic resonance imaging (MRI) lesions within central autonomic network brain regions' associations with PSH-AM scores in a large critically ill TBI cohort also identified susceptibility-weighted imaging (SWI) lesions in the corpus

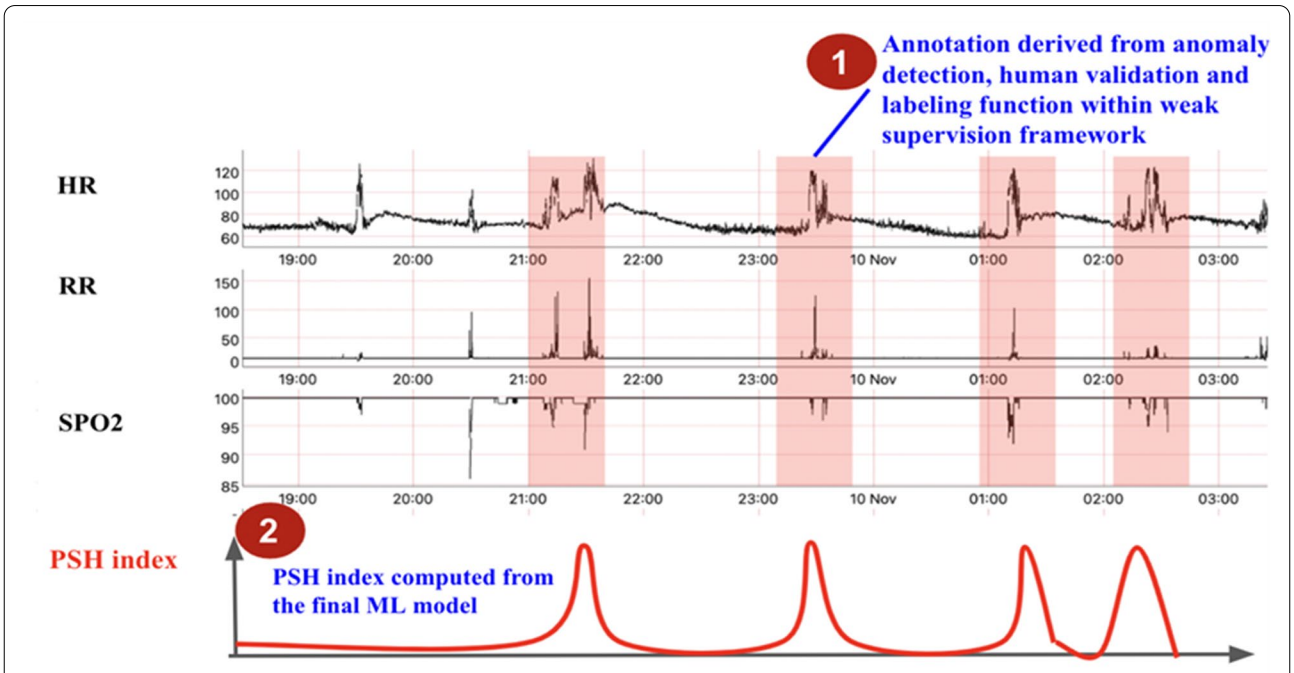

Fig. 4 Anomaly detection for identification of PSH events. This plot illustrates an example of multivariate anomaly detection framework we are exploring for identifying PSH events from continuous physiological time series data. The top panel presents time plots of HR, RR, and oxygen saturation overlaid with abnormal episodes (red-colored band) obtained from a combination of anomaly detection methods, human validation, and labeling functions within a weak supervision framework. The bottom panel illustrates a continuous PSH index once the supervised machine learning model is built that contrasts the PSH and non-PSH periods. *HR* heart rate, *ML* machine learning, *PSH* paroxysmal sympathetic hyperactivity, *RR* respiratory rate, *SPO2* oxygen saturation (color figure online)

callosum (as in Fig. 4c) and T2 flair lesions in the medial temporal lobes as independently associated with higher PSH diagnostic likelihood [68]. Neuroimaging, like physiologic studies, have suffered from imprecise and subjective methods for identifying and quantifying PSH; a quantitative PSH index could aid in neuroanatomic phenotyping of this prototypical syndrome of dysautonomia that may represent a modifiable risk factor for poor TBI [68] outcome.

Predicting Neurological Decline

Traumatic Brain Injury (TBI)

Since the pioneering work of Dr. R Adams Cowley in the mid-twentieth century, acute trauma care has stressed the importance of rapid assessment and skilled treatment during the "golden hour" [69], when interventions are most likely to prevent long-term morbidity and mortality. Although monitoring techniques have greatly aided the rapid ability to dynamically evaluate for secondary decline (e.g., hemorrhage), our current ability to acutely assess for secondary ND after TBI remain rudimentary. Initial risk stratification after injury, particularly prior to neuroimaging, is based on clinical judgment, clinical examination, and assessment of static vital signs [70], which only provide limited information. Additional essential information can be derived from the analysis of continuous vital sign data and waveform analysis during the acute resuscitation period.

In combination with routine clinical assessments in the first hour after injury, continuous vital sign monitoring for variability and waveform feature analyses from either the ECG or PPG can be used to reliably predict early (< 48 h after injury) neurological decline (ND) in patients with TBI. As an initial analysis, we found that without regards to patient age, sex, GCS, or initial set of vital signs, PPG and ECG analyses alone during the first 15 min of acute resuscitation were equivalent to clinical models that incorporated age, initial GCS, and sex to predict ND after TBI [41]. Moreover, a model combining PPG data with clinical characteristics within 15 and 60 min (golden hour) after arrival yielded an improved prediction power for ND. These analyses reflect the great potential of assessing the physiological state by utilizing continuous vital sign data to enhance the clinical assessment.

As discussed previously, HRV has been used in studies of neurologic disorders [13, 27] as a marker of the function of the ANS [71]. Specific to TBI, dysautonomia has been closely linked to increased ICP or decreased cerebral perfusion pressure [72]. The pulse oximeter is a commonly used sensor that can provide rich data by generation of a PPG waveform providing additional information on HR, oxygen saturation, and RR [73]. The PPG peaks correspond to the R peaks from ECG, therefore, the peak-peak interval from PPG can be used as an alternative to the NN interval calculated from ECG recordings. Lu et al. [74] found PPG variability was highly correlated to HRV and could serve as an alternative measurement. Several studies have correlated similar physiological measurements with autonomic changes in patients with TBI with the severity of injury and, association with increased ICP [20, 75, 76] as well as overall morbidity and mortality [20, 76, 77].

This novel approach for early detection of ND uses continuous ECG and PPG data from the first minutes of arrival, prior to ICP monitoring and CT imaging, further signifying the viability of physiologic and waveform analysis as a robust early marker in the resuscitation phase. It is important to note that within 15 min of arrival, patients are still undergoing physical examination and assessment, and not under the influence of sedatives or analgesics that may confound the signal from the continuous vital sign data collection. The ability to accurately discern a risk for ND early in the acute resuscitation phase may provide for an opportunity to develop targeted interventions to mitigate secondary injury, including rapid triage for timely, definitive treatment for patients with TBI. We are currently validating our preliminary findings in both retrospective and prospective cohort studies (NCT05084352).

Large Hemispheric Infarction (LHI)

Patients with LHI, as defined by infarct of the majority or complete distribution of the middle cerebral artery territory, account for less than 10% of acute ischemic strokes [78]. However, approximately half of patients with LHI develop malignant cerebral edema (MCE) which is associated with a mortality rate between 40 and 80% [79–81]. Early ND is commonly seen in patients with MCE due to LHI and is associated with increased mortality [82–85]. Swift identification of patients at risk for early ND and MCE is essential to ensure timely targeted medical and potentially surgical interventions to mitigate secondary brain injury. Both nonmodifiable (e.g., diabetes mellitus, prestroke modified Rankin score, initial National Institutes of Health Stroke Scale Score [NIHSS], stroke volume on MRI) and modifiable (e.g., number of passes during endovascular treatment) factors have been identified as predictors of early ND and evolution to MCE [86, 87]. More recently studies have found autonomic dysfunction as defined by HRV to predict poor outcome [88] and to be an independent risk factor for early ND [89] in acute ischemic stroke. Physiologic data are therefore a potentially rich resource for assessing autonomic integrity in patients with LHI that may serve as an early predictor for patients who will develop early ND and MCE.

Central control of the ANS is performed by a complex neural network of several cortical and subcortical areas as described previously. The insular cortex, often affected in patients with acute ischemic stroke and particularly LHI, plays a vital role in cardiac modulation via the heart-brain axis. Both rat and human experiments have shown that cardiac afferent fibers travel through the thalamus to the posterior insula with integration of information from the rostroventral insula [6]. Stimulation of the rostral versus caudal insula has shown varying effects on HR with rostral posterior insular stimulation resulting in tachycardia and caudal posterior insular stimulation resulting in bradycardia [90]. The posterior insula has also been implicated in worsening heart block and ventricular arrhythmias leading to death in rat models suggesting the rostro-caudal axis is of particular importance [91].

Though the cardiac effects of the rostro-caudal axis have been more clearly defined, lateralization of sympathetic and parasympathetic control has shown mixed findings in both animal and human studies. Historically, the right insula was thought to be responsible for sympathetic control and the left insula for parasympathetic control [92, 93]. Recent studies have not supported a clear delineation of laterality for sympathetic and parasympathetic control of the insula with insular stimulations in humans showing no difference in tachy-arrhythmias or brady-arrhythmias between the right and left insular cortices [94]. However, insular subregions have shown laterality preference with tachycardia more often evoked by stimulation of the right ventral posterior insula and the left dorsal posteromedial insula whereas bradycardia was evoked by stimulations of the right dorsal insula and the left ventral insula [94]. The insular cortex as demonstrated in animal and human studies provides a lens into potential ANS dysfunction and presents a unique opportunity for identifying early ND and MCE in patients with LHI.

As seen in Fig. 5, using our vital sign viewer, patients with LHI can have a noticeable change in their HR preceding a herniation event, part of the Cushing triad [95], presenting a potential window of opportunity for prediction and early goal-directed management. When filtering

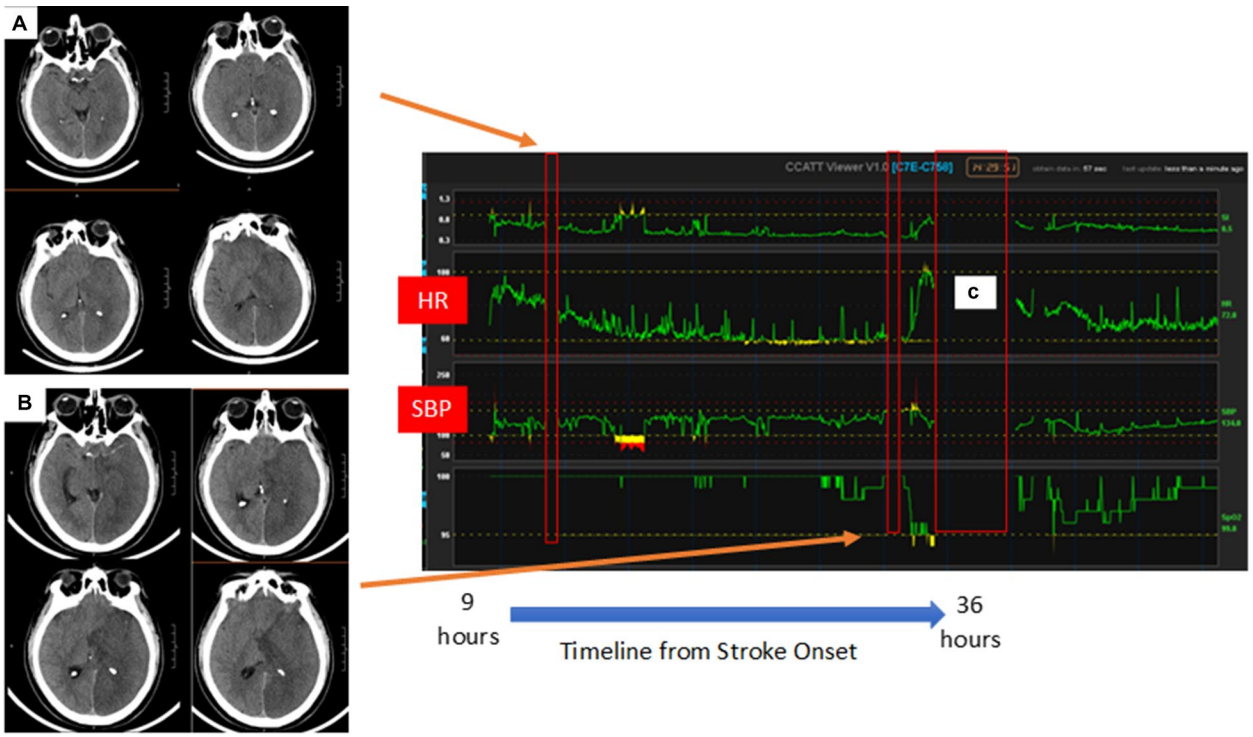

Fig. 5 Changes in physiological state related to cerebral edema. A patient presenting at the Neuro-ICU with a large hemispheric stroke after failed thrombectomy for a left middle cerebral artery occlusion. At time of the initial CT, early signs of cerebral edema are present (**a**) but the clinical examination does not change until nearly 24 hours later, when a subsequent CT scan is performed demonstrating radiographic herniation (**b**). The patient is subsequently taken to the operating room for decompressive hemicraniectomy (**c**). As noted in our vital sign viewer, progressive bradycardia in the hours preceding the clinical and radiographic herniation (between **a** and **b**) is visually apparent, representing a window of opportunity for physiologically based early warning signal. *CT* computed tomography, *HR* heart rate, *Neuro-ICU* neuroscience intensive care unit, *SBP* systolic blood pressure (color figure online)

the signal to monitor HRV and waveform changes, one can observe the initial subtle changes within hours of injury that continue to evolve over subsequent hours. In our preliminary analyses, we have found that changes in the LF/HF ratio within 12 h of stroke onset may be an independent predictor of early ND, and RR interval was an independent predictor of MCE [96]. Our findings suggest that even within the first 3 h of hemodynamic monitoring, early identification of autonomic dysfunction via HRV may provide a window of opportunity to impact therapeutic approaches toward early ND and MCE.

Spinal Cord Injury (SCI)

Despite advances in acute trauma, neurosurgical, ICU, and rehabilitative care, traumatic SCI remains a costly multisystemic disease with limited effective treatment options. Disability from SCI arises most obviously from loss of motor and sensory function, which is typically measured and classified by the American Spinal Injury Association (ASIA) scoring system in clinical and research practice [97]. ASIA scores provide important prognostic information that may guide management. For example, early ASIA motor scores may guide the decision to pursue early tracheostomy [98], and discharge ASIA impairment scores help guide long-term prognosis for recovery. However, ASIA scores do not measure SCI-related dysautonomia, which results from damage to descending control of efferent sympathetic nerves and may clinically manifest as neurogenic shock, autonomic dysreflexia, orthostatic hypotension, arrythmias, and widespread deleterious effects on visceral organ system function [99]. Studies have suggested that autonomic injury severity may be discordant with sensory and motor injury severity [100]. In recognizing the importance of the ANS in SCI care and prognostication, the International Standards to document remaining Autonomic Function after Spinal Cord Injury was first developed in 2009 [101]. Analogous to ASIA scoring and the PSH-AM, its Autonomic Standards Assessment Form allows for characterization and documentation of clinical manifestations of specific autonomic functions in patients with SCI, and in doing so, may provide standards for physiologic data correlation.

Quantitative approaches to autonomic dysfunction using physiologic data in the acute phase after SCI may vary depending on the goal and hypothesis of research. As in the PSH example, weakly supervised machine learning may be employed for early detection and monitoring of deleterious and potentially intervenable forms of SCI-associated dysautonomia. Physiologic data also may be modeled in conjunction with clinical, radiographic, and neuroanatomic injury data, such as level of injury and intramedullary lesion length, for better multimodal injury phenotyping. Loss of LF power has most commonly been associated with reduced sympathetic control in cervical SCI [100, 102], for example. Alternatively, as in our ND examples, physiologic data may be used to model and predict clinical endpoints. As of yet, no large studies have evaluated the prognostic value of early markers of dysautonomia on short and long-term multisystemic and global outcomes after SCI. Given that dysautonomia, like sensorimotor dysfunction, is an important contributor to morbidity and mortality after SCI, we hypothesize that early measures of dysautonomia may improve prediction of clinically meaningful outcomes and generate hypotheses for targeted therapeutic interventions.

Challenges/Future Directions

Additional conditions that have used advanced techniques to monitor ANS function include subarachnoid hemorrhage, multiorgan dysfunction syndrome, sepsis, and cardiac arrest [103, 104]. Applications are not limited to those previously studied and discussed; profound ANS changes occur in other neurologic diseases often encountered in the ICU, including autoimmune (e.g., NMDA) encephalitis [105], Guillain Barre Syndrome [106], and status epilepticus [107]. However, big data and machine learning approaches to dysautonomia in these scenarios will be limited by their rarity and may necessitate multicenter collaborations.

The assessment of autonomic function in the critically ill provides unique information concerning pathogenesis, treatment strategies, and prognosis; however, additional foundational data are needed to refine analyses to be readily available for routine clinical use. The highly sensitive nature of ANS dysfunction across all injury types can result in a lack of disease-specific signal, making discerning relevant signals difficult. It is unclear whether final common pathways or disease-specific physiologic phenotypes will be of greater clinical use.

Beyond the consensus definitions (e.g., the Task Force of the European Society of Cardiology and the North American Society of Pacing and Electrophysiology [13]), there is also a lack of uniformity regarding timing, depth and duration of ANS signal changes that are deemed clinically relevant. Moreover, many concomitant interventions (nonpharmacological and pharmacological) have a profound impact on the ANS signal, highlighting the importance of developing real-time data annotation. Integrated information systems that incorporate clinical and physiologic data are needed. At present, physiologic data monitoring and storage systems exist outside of the electronic medical record, and clinical annotation is primarily performed manually and post hoc for model development. Real-time, automated integration of medication administration and common interventions such as

endotracheal intubation, bedside procedures, and surgeries, is essential to enhance the generalizability and clinical validity of models. Additional relevant bedside data streams from automated pupillometry, galvanic skin response, EEG, invasive neuromonitoring, as well as laboratory studies can be used in targeted patient populations at risk for ANS dysfunction or ND to provide more nuanced and complementary information regarding dynamic sympathetic/ parasympathetic balance.

Conclusions

The complex and dynamic changes that occur as a universal response to neurological injury may go undetected in standard practice, in which hourly vital signs, clinical examinations, laboratory, and other low-resolution data requires human interpretation for clinical decision making. Machine-based, high-resolution ANS monitoring may extend clinicians abilities to detect meaningful physiologic changes during critical periods for medical or surgical intervention. Although promising work in this area applied to TBI and LHI has been discussed, we believe that continued study and collaborative innovations in technology and data-analytic approaches are needed to fully leverage continuous vital sign measurements of ANS dysfunction to improve clinical care of patients with acute brain injury.

Author details

[1] Program in Trauma, University of Maryland School of Medicine, Baltimore, MD, USA. [2] Department of Neurology, University of Maryland School of Medicine, Baltimore, MD, USA. [3] Department of Anesthesiology, University of Maryland School of Medicine, Baltimore, MD, USA. [4] Department of Epidemiology and Public Health, University of Maryland School of Medicine, Baltimore, MD, USA. [5] Department of Information Systems, College of Engineering and Information Technology, University of Maryland Baltimore County, Baltimore, MD, USA. [6] Enroute Care Division, Department of Aeromedical Research, United States Air Force School of Aerospace Medicine, Wright-Patterson Air Force Base, Dayton, OH, USA. [7] Shock Trauma Neurocritical Care, University of Maryland Medical Center, 22 S. Greene Street, G7k19, Baltimore, MD 21218, USA.

Author Contributions

NB, JP, MP, PH, and SY: concept and design of the study, analysis of data, writing of the article. HC and LC: analysis of data and critical revision. RF: data collection, administrative support, and critical revision. CM and GP: analysis of data, important intellectual content, and critical revision. The final manuscript was approved by all authors.

Source of Support

NB, PH, and SY received funding support from United States Air Force (USAF) (FA8650-18-2-6H18). NB received funding from National Institute of Neurological Disorders and Stroke/National Institutes of Health (NINDS/NIH) (NS10505503).

Conflicts of interest

The authors declare that they have no conflicts of interest.

Ethical Approval/Informed Consent

This is a review article and does not contain new data necessitating ethical approval.

Publisher's Note

Received: 10 December 2021 Accepted: 14 March 2022

References

1. Karemaker JM. An introduction into autonomic nervous function. Physiol Meas. 2017;38:R89–118.
2. Agarwal SK, Calaresu FR. Electrical stimulation of nucleus tractus solitarius excites vagal preganglionic cardiomotor neurons of the nucleus ambiguus in rats. Brain Res. 1992;574:320–4.
3. Kimmerly DS. A review of human neuroimaging investigations involved with central autonomic regulation of baroreflex-mediated cardiovascular control. Auton Neurosci. 2017;207:10–21.
4. Palma JA, Benarroch EE. Neural control of the heart: recent concepts and clinical correlations. Neurology. 2014;83:261–71.
5. Shoemaker JK, Goswami R. Forebrain neurocircuitry associated with human reflex cardiovascular control. Front Physiol. 2015;6:240.
6. Tahsili-Fahadan P, Geocadin RG. Heart–brain axis: effects of neurologic injury on cardiovascular function. Circ Res. 2017;120:559–72.
7. Dimitri GM, Agrawal S, Young A, Donnelly J, Liu X, Smielewski P, et al. A multiplex network approach for the analysis of intracranial pressure and heart rate data in traumatic brain injured patients. Appl Netw Sci. 2017;2:29.
8. Dimitri GM, Agrawal S, Young A, Donnelly J, Liu X, Smielewski P, et al. Simultaneous transients of intracranial pressure and heart rate in traumatic brain injury: methods of analysis. Acta Neurochir Suppl. 2018;126:147–51.
9. Dimitri GM, Beqiri E, Placek MM, Czosnyka M, Stocchetti N, Ercole A, et al. Modeling brain–heart crosstalk information in patients with traumatic brain injury. Neurocrit Care. 2021. https://doi.org/10.1007/s12028-021-01353-7.
10. Wee BYH, Lee JH, Mok YH, Chong SL. A narrative review of heart rate and variability in sepsis. Ann Transl Med. 2020;8:768.
11. Brinza C, Floria M, Covic A, Burlacu A. Measuring heart rate variability in patients admitted with st-elevation myocardial infarction for the prediction of subsequent cardiovascular events: a systematic review. Medicina (Kaunas). 2021;57:1021.
12. Cooke WH, Salinas J, Convertino VA, Ludwig DA, Hinds D, Duke JH, et al. Heart rate variability and its association with mortality in prehospital trauma patients. J Trauma. 2006;60:363–70 (**discussion 370**).
13. Task Force of the European Society of Cardiology and the North American Society of Pacing and Electrophysiology. Heart rate variability. Standards of measurement, physiological interpretation, and clinical use. Eur Heart J. 1996;17:354–81.
14. Nolan J, Batin PD, Andrews R, Lindsay SJ, Brooksby P, Mullen M, et al. Prospective study of heart rate variability and mortality in chronic heart failure: results of the united kingdom heart failure evaluation and assessment of risk trial (UK-heart). Circulation. 1998;98:1510–6.
15. Toweill D, Sonnenthal K, Kimberly B, Lai S, Goldstein B. Linear and nonlinear analysis of hemodynamic signals during sepsis and septic shock. Crit Care Med. 2000;28:2051–7.
16. Garrard CS, Kontoyannis DA, Piepoli M. Spectral analysis of heart rate variability in the sepsis syndrome. Clin Auton Res. 1993;3:5–13.
17. Heinroth KM, Kuhn C, Stache N. Attenuated heart rate variability in septic and non septic shock multiple organ dysnfunction syndrome. Intensvivmed. 1993;36:436–45.
18. Dunser MW, Hasibeder WR. Sympathetic overstimulation during critical illness: adverse effects of adrenergic stress. J Intensive Care Med. 2009;24:293–316.
19. Baguley IJ, Nicholls JL, Felmingham KL, Crooks J, Gurka JA, Wade LD. Dysautonomia after traumatic brain injury: a forgotten syndrome? J Neurol Neurosurg Psychiatry. 1999;67:39–43.
20. Biswas AK, Scott WA, Sommerauer JF, Luckett PM. Heart rate variability after acute traumatic brain injury in children. Crit Care Med. 2000;28:3907–12.

21. Haji-Michael PG, Vincent JL, Degaute JP, van de Borne P. Power spectral analysis of cardiovascular variability in critically ill neurosurgical patients. Crit Care Med. 2000;28:2578–83.
22. Maas AIR, Menon DK, Adelson PD, Andelic N, Bell MJ, Belli A, et al. Traumatic brain injury: integrated approaches to improve prevention, clinical care, and research. Lancet Neurol. 2017;16:987–1048.
23. Monsour M, Ebedes D, Borlongan CV. A review of the pathology and treatment of tbi and ptsd. Exp Neurol. 2022;351:114009.
24. Valenza G, Toschi N, Barbieri R. Uncovering brain–heart information through advanced signal and image processing. Philos Trans A Math Phys Eng Sci. 2016;374:20160020.
25. Hu PF, Yang S, Li HC, Stansbury LG, Yang F, Hagegeorge G, et al. Reliable collection of real-time patient physiologic data from less reliable networks: a "monitor of monitors" system (moms). J Med Syst. 2017;41:3.
26. Acharya UR, Joseph KP, Kannathal N, Lim CM, Suri JS. Heart rate variability: a review. Med Biol Eng Comput. 2006;44:1031–51.
27. Ernst G. Heart rate variability. London: Springer; 2014.
28. Oka H. Heart rate variability and neurological disorders. Clinical assessment of the autonomic nervous system. Tokyo: Springer; 2017. p. 179–97.
29. Goodman BB, David VD. Autonomic nervous system dysfunction in concussion. Neurology. 2013;80:P01-P265.
30. Baguley IJ, Heriseanu RE, Felmingham KL, Cameron ID. Dysautonomia and heart rate variability following severe traumatic brain injury. Brain Inj. 2006;20:437–44.
31. Garcia D. Robust smoothing of gridded data in one and higher dimensions with missing values. Comput Stat Data Anal. 2010;54:1167–78.
32. Press WH, Teukolsky SA, Vetterling WT, Flannery BP. Chapter 14: Statistical description of data. Cambridge: Cambridge University Press; 2007.
33. Palacios VJPF, Fernández-Delgado J, Felix M, Barro SP. Time-frequency analysis of heart-rate variability. IEEE Eng Med Biol. 1997;16:119–26.
34. Pan J, Tompkins WJ. A real-time QRS detection algorithm. IEEE Trans Biomed Eng. 1985;32:230–6.
35. Malliani A, Pagani M, Lombardi F, Cerutti S. Cardiovascular neural regulation explored in the frequency domain. Circulation. 1991;84:482–92.
36. Delgado-Bonal AMA. Approximate entropy and sample entropy: a comprehensive tutorial. Entropy. 2019;21:541.
37. Henriques TRM, Castro TA, Antunes L, Costa-Santos LC. Nonlinear methods most applied to heart rate time series: a review. Entropy (Basel). 2020;22:309.
38. Shaffer F, Ginsberg JP. An overview of heart rate variability metrics and norms. Front Public Health. 2017;5:258.
39. Melillo P, Izzo R, Orrico A, Scala P, Attanasio M, Mirra M, et al. Automatic prediction of cardiovascular and cerebrovascular events using heart rate variability analysis. PLoS ONE. 2015;10:e0118504.
40. Parimi N, Hu PF, Mackenzie CF, Yang S, Bartlett ST, Scalea TM, et al. Automated continuous vital signs predict use of uncrossed matched blood and massive transfusion following trauma. J Trauma Acute Care Surg. 2016;80:897–906.
41. Melinosky C, Yang S, Hu P, Li H, Miller CHT, Khan I, et al. Continuous vital sign analysis to predict secondary neurological decline after traumatic brain injury. Front Neurol. 2018;9:761.
42. Czosnyka M, Smielewski P, Kirkpatrick P, Menon DK, Pickard JD. Monitoring of cerebral autoregulation in head-injured patients. Stroke. 1996;27:1829–34.
43. Czosnyka M, Miller C. Participants in the international multidisciplinary consensus conference on multimodality M. Monitoring of cerebral autoregulation. Neurocrit Care. 2014;21(Suppl 2):S95–102.
44. Baguley IJ, Perkes IE, Fernandez-Ortega JF, Rabinstein AA, Dolce G, Hendricks HT, et al. Paroxysmal sympathetic hyperactivity after acquired brain injury: consensus on conceptual definition, nomenclature, and diagnostic criteria. J Neurotrauma. 2014;31:1515–20.
45. Meyfroidt G, Baguley IJ, Menon DK. Paroxysmal sympathetic hyperactivity: the storm after acute brain injury. Lancet Neurol. 2017;16:721–9.
46. Marehbian J, Muehlschlegel S, Edlow BL, Hinson HE, Hwang DY. Medical management of the severe traumatic brain injury patient. Neurocrit Care. 2017;27:430–46.
47. Podell JE, Miller SS, Jaffa MN, Pajoumand M, Armahizer M, Chen H, et al. Admission features associated with paroxysmal sympathetic hyperactivity after traumatic brain injury: a case–control study. Crit Care Med. 2021;49:e989–1000.
48. Rabinstein AA. Paroxysmal sympathetic hyperactivity in the neurological intensive care unit. Neurol Res. 2007;29:680–2.
49. Samuel S, Lee M, Brown RJ, Choi HA, Baguley IJ. Incidence of paroxysmal sympathetic hyperactivity following traumatic brain injury using assessment tools. Brain Inj. 2018;32:1115–21.
50. van Eijck MM, Sprengers MOP, Oldenbeuving AW, de Vries J, Schoonman GG, Roks G. The use of the psh-am in patients with diffuse axonal injury and autonomic dysregulation: a cohort study and review. J Crit Care. 2019;49:110–7.
51. Lucca LF, De Tanti A, Cava F, Romoli A, Formisano R, Scarponi F, et al. Predicting outcome of acquired brain injury by the evolution of paroxysmal sympathetic hyperactivity signs. J Neurotrauma. 2021;38:1988–94.
52. Baguley IJ, Nott MT, Slewa-Younan S, Heriseanu RE, Perkes IE. Diagnosing dysautonomia after acute traumatic brain injury: evidence for overresponsiveness to afferent stimuli. Arch Phys Med Rehabil. 2009;90:580–6.
53. Hinson HE, Puybasset L, Weiss N, Perlbarg V, Benali H, Galanaud D, et al. Neuroanatomical basis of paroxysmal sympathetic hyperactivity: a diffusion tensor imaging analysis. Brain Inj. 2015;29:455–61.
54. Kramer AA, Sebat F, Lissauer M. A review of early warning systems for prompt detection of patients at risk for clinical decline. J Trauma Acute Care Surg. 2019;87:S67–73.
55. Datta DPM, Chiu J, Watson GS, Bywater JP, Barnes L, et al. Improving classification through weak supervision in context-specific conversational agent development for teacher education. http://arxiv.org/abs/2010.127102020.
56. Ratner A, Bach SH, Ehrenberg H, Fries J, Wu S, Re C. Snorkel: rapid training data creation with weak supervision. Proc VLDB Endow. 2017;11:269–82.
57. Liu M. (2019) Weak supervision and active learning for natural language processing (PhD Thesis); Monash University.
58. Settles, B. (2009). Active Learning Literature Survey.
59. Jalali LJR. Event mining for explanatory modeling. New York: ACM; 2021.
60. Chalapathy R, Chawla S. Deep learning for anomaly detection: a survey; 2019. http://arxiv.org/abs/1901.03407
61. Gelatti GJ, Carvalho A, Rodrigues P. Learning representations from healthcare time series data for unsupervised anomaly detection. In: 2019 IEEE international conference on big data and smart computing (BigComp); 2019.
62. Gelatti GJ, Carvalho A, Rodrigues P. Learning representations from healthcare time series data for unsupervised anomaly detection. In: 2019 IEEE international conference on big data and smart computing (BigComp).
63. Pereira U, Brunel N. Unsupervised learning of persistent and sequential activity. Front Comput Neurosci. 2019;13:97.
64. Guillame-Bert M, Dubrawski A. Classification of time sequences using graphs of temporal constraints. J Mach Learn Res. 2017;1–34.
65. Wang Z, Yan W, Oates T. Time series classification from scratch with deep neural networks: a strong baseline. In: 2017 international joint conference on neural networks (IJCNN); 2017.
66. Penfield W. Epilepsy and the functional anatomy of the human brain. London: J & A Churchill Ltd; 1954. p. 412–37.
67. Lv LQ, Hou LJ, Yu MK, Qi XQ, Chen HR, Chen JX, et al. Prognostic influence and magnetic resonance imaging findings in paroxysmal sympathetic hyperactivity after severe traumatic brain injury. J Neurotrauma. 2010;27:1945–50.
68. Podell J, Parikh G, Miller S, Tripathi H, Zhuo J, Roys S, Schwartzbauer G, Gullapalli R, Badjatia N. Acute traumatic brain injury magnetic resonance imaging lesions associated with paroxysmal sympathetic hyperactivity diagnostic likelihood. In: 19th annual meeting of the neurocritical care society; 2021.
69. Cowley RA. Resuscitaion and stabilization of major multiple trauma patients in a trauma center environment. Clin Med. 1976;83:16–22.
70. Lingsma HF, Roozenbeek B, Steyerberg EW, Murray GD, Maas AI. Early prognosis in traumatic brain injury: From prophecies to predictions. Lancet Neurol. 2010;9:543–54.
71. Rajendra Acharya U, Paul Joseph K, Kannathal N, Lim CM, Suri JS. Heart rate variability: a review. Med Biol Eng Comput. 2006;44:1031–51.
72. Goldstein B, Kempski MH, DeKing D, Cox C, DeLong DJ, Kelly MM, et al. Autonomic control of heart rate after brain injury in children. Crit Care Med. 1996;24:234–40.

73. Allen J. Photoplethysmography and its application in clinical physiological measurement. Physiol Meas. 2007;28:R1-39.
74. Lu S, Zhao H, Ju K, Shin K, Lee M, Shelley K, et al. Can photoplethysmography variability serve as an alternative approach to obtain heart rate variability information? J Clin Monit Comput. 2008;22:23–9.
75. Kahraman S, Dutton RP, Hu P, Stansbury L, Xiao Y, Stein DM, et al. Heart rate and pulse pressure variability are associated with intractable intracranial hypertension after severe traumatic brain injury. J Neurosurg Anesthesiol. 2010;22:296–302.
76. Mowery NT, Norris PR, Riordan W, Jenkins JM, Williams AE, Morris JA Jr. Cardiac uncoupling and heart rate variability are associated with intracranial hypertension and mortality: a study of 145 trauma patients with continuous monitoring. J Trauma. 2008;65:621–7.
77. Winchell RJ, Hoyt DB. Analysis of heart-rate variability: a noninvasive predictor of death and poor outcome in patients with severe head injury. J Trauma. 1997;43:927–33.
78. Heinsius T, Bogousslavsky J, Van Melle G. Large infarcts in the middle cerebral artery territory. Etiology and outcome patterns. Neurology. 1998;50:341–50.
79. Thomalla G, Hartmann F, Juettler E, Singer OC, Lehnhardt FG, Kohrmann M, et al. Prediction of malignant middle cerebral artery infarction by magnetic resonance imaging within 6 hours of symptom onset: a prospective multicenter observational study. Ann Neurol. 2010;68:435–45.
80. Liebeskind DS, Juttler E, Shapovalov Y, Yegin A, Landen J, Jauch EC. Cerebral edema associated with large hemispheric infarction. Stroke. 2019;50:2619–25.
81. Hacke W, Schwab S, Horn M, Spranger M, De Georgia M, von Kummer R. 'Malignant' middle cerebral artery territory infarction: clinical course and prognostic signs. Arch Neurol. 1996;53:309–15.
82. Siegler JE, Boehme AK, Kumar AD, Gillette MA, Albright KC, Martin-Schild S. What change in the national institutes of health stroke scale should define neurologic deterioration in acute ischemic stroke? J Stroke Cerebrovasc Dis. 2013;22:675–82.
83. Seners P, Turc G, Tisserand M, Legrand L, Labeyrie MA, Calvet D, et al. Unexplained early neurological deterioration after intravenous thrombolysis: incidence, predictors, and associated factors. Stroke. 2014;45:2004–9.
84. Davalos A, Toni D, Iweins F, Lesaffre E, Bastianello S, Castillo J. Neurological deterioration in acute ischemic stroke: potential predictors and associated factors in the European cooperative acute stroke study (ECASS) I. Stroke. 1999;30:2631–6.
85. Arenillas JF, Rovira A, Molina CA, Grive E, Montaner J, Alvarez-Sabin J. Prediction of early neurological deterioration using diffusion- and perfusion-weighted imaging in hyperacute middle cerebral artery ischemic stroke. Stroke. 2002;33:2197–203.
86. Simard JM, Sahuquillo J, Sheth KN, Kahle KT, Walcott BP. Managing malignant cerebral infarction. Curr Treat Options Neurol. 2011;13:217–29.
87. Girot JB, Richard S, Gariel F, Sibon I, Labreuche J, Kyheng M, et al. Predictors of unexplained early neurological deterioration after endovascular treatment for acute ischemic stroke. Stroke. 2020;51:2943–50.
88. Chen CH, Huang PW, Tang SC, Shieh JS, Lai DM, Wu AY, et al. Complexity of heart rate variability can predict stroke-in-evolution in acute ischemic stroke patients. Sci Rep. 2015;5:17552.
89. He L, Wang J, Zhang L, Zhang X, Dong W, Yang H. Decreased fractal dimension of heart rate variability is associated with early neurological deterioration and recurrent ischemic stroke after acute ischemic stroke. J Neurol Sci. 2019;396:42–7.
90. Oppenheimer SM, Cechetto DF. Cardiac chronotropic organization of the rat insular cortex. Brain Res. 1990;533:66–72.
91. Oppenheimer SM, Wilson JX, Guiraudon C, Cechetto DF. Insular cortex stimulation produces lethal cardiac arrhythmias: a mechanism of sudden death? Brain Res. 1991;550:115–21.
92. Ruiz Vargas E, Soros P, Shoemaker JK, Hachinski V. Human cerebral circuitry related to cardiac control: a neuroimaging meta-analysis. Ann Neurol. 2016;79:709–16.
93. Oppenheimer SM, Gelb A, Girvin JP, Hachinski VC. Cardiovascular effects of human insular cortex stimulation. Neurology. 1992;42:1727–32.
94. Chouchou F, Mauguiere F, Vallayer O, Catenoix H, Isnard J, Montavont A, et al. How the insula speaks to the heart: cardiac responses to insular stimulation in humans. Hum Brain Mapp. 2019;40:2611–22.
95. Dinallo S, Waseem M. Cushing reflex. Treasure Island: Statpearls; 2021.
96. Pergakis MB, Miller S, Tripathi H, Hu P, Parikh G, Morris N, Chang W, Motta M, Chaturvedi S, Jindal G, Simard JM, Badjatia N. Association between heart rate variability and secondary brain injury in patients with large hemispheric infarct. In: Neurocritical care society 18th annual meeting; 2020.
97. Rupp R, Biering-Sorensen F, Burns SP, Graves DE, Guest J, Jones L, et al. International standards for neurological classification of spinal cord injury: revised 2019. Top Spinal Cord Injury Rehabil. 2021;27:1–22.
98. Menaker J, Kufera JA, Glaser J, Stein DM, Scalea TM. Admission Asia motor score predicting the need for tracheostomy after cervical spinal cord injury. J Trauma Acute Care Surg. 2013;75:629–34.
99. Biering-Sorensen F, Biering-Sorensen T, Liu N, Malmqvist L, Wecht JM, Krassioukov A. Alterations in cardiac autonomic control in spinal cord injury. Auton Neurosci. 2018;209:4–18.
100. Lucci VM, Inskip JA, McGrath MS, Ruiz I, Lee R, Kwon BK, et al. Longitudinal assessment of autonomic function during the acute phase of spinal cord injury: use of low-frequency blood pressure variability as a quantitative measure of autonomic function. J Neurotrauma. 2021;38:309–21.
101. Krassioukov A, Biering-Sorensen F, Donovan W, Kennelly M, Kirshblum S, Krogh K, et al. International standards to document remaining autonomic function after spinal cord injury. J Spinal Cord Med. 2012;35:201–10.
102. Inoue K, Miyake S, Kumashiro M, Ogata H, Yoshimura O. Power spectral analysis of heart rate variability in traumatic quadriplegic humans. Am J Physiol. 1990;258:H1722-1726.
103. Johnston BW, Barrett-Jolley R, Krige A, Welters ID. Heart rate variability: measurement and emerging use in critical care medicine. J Intensive Care Soc. 2020;21:148–57.
104. Uryga A, Burzynska M, Tabakow P, Kasprowicz M, Budohoski KP, Kazimierska A, et al. Baroreflex sensitivity and heart rate variability are predictors of mortality in patients with aneurysmal subarachnoid haemorrhage. J Neurol Sci. 2018;394:112–9.
105. Yan L, Zhang S, Huang X, Tang Y, Wu J. Clinical study of autonomic dysfunction in patients with anti-nmda receptor encephalitis. Front Neurol. 2021;12:609750.
106. Zaeem Z, Siddiqi ZA, Zochodne DW. Autonomic involvement in Guillain-Barre syndrome: an update. Clin Auton Res. 2019;29:289–99.
107. Oduah MT, Iwanowski P. Cardiovascular complications of epileptic seizures. Epilepsy Behav. 2020;111:107185.